Time-dependent analytical *R*-matrix approach for strong-field dynamics. I. One-electron systems

Lisa Torlina and Olga Smirnova
Max Born Institute, Max Born Strasse 2a, 12489 Berlin, Germany
(Received 2 May 2012; published 5 October 2012)

We develop a flexible analytical approach to describe strong-field dynamics in atoms and molecules. The approach is based on the ideas of the *R*-matrix method. Here, we illustrate and validate our approach by applying it to systems with one active electron bound by the Coulomb potential and benchmark our results against the standard theory of Perelomov, Popov, and Terent'ev [Sov. Phys. JETP **23**, 924 (1966)]. We discuss corrections to the ionization amplitude associated with the interplay of the Coulomb potential and the laser field on the sub-laser cycle time scale and the shape of the tunneling wave packets associated with different instants of ionization.

DOI: 10.1103/PhysRevA.86.043408 PACS number(s): 32.80.Rm, 42.50.Hz, 33.80.Wz

I. INTRODUCTION

One of the most powerful ideas in describing scattering and ionization in multielectron systems is embedded in the *R*-matrix method [1], which partitions the space into outer and inner regions. This partitioning reflects different dynamics of the two interacting subsystems, for example, ion and liberated electron in the case of one-electron ionization. The outer region corresponds to the electron being sufficiently far away from the ionic core. The words "*sufficiently far*" imply that a simplified description of the electron-core interaction is possible, for example, neglecting electron exchange. Dynamics in the inner region, on the other hand, could be very complex, but the limited volume of the inner region offers important simplifications, such as the possibility to use the theoretical machinery already developed for bound states of multielectron systems.

The goal of this paper is to develop an analytical description that would take advantage of the *R*-matrix concept: the analytical *R*-matrix method (ARM). When it comes to analytical or semianalytical methods in strong laser fields, dividing the space into inner and outer regions also offers benefits. Indeed, the root difficulty of analytical approaches in strong-field dynamics is the need to include both types of electron interactions—with the laser field and with the ionic core—beyond the standard time-dependent perturbation theory. This difficulty is naturally resolved in the outer region, where the electron is sufficiently far away from the Coulomb singularity of the ionic core. In this region, the strong-field eikonal-Volkov approximation [2] becomes quite accurate [3]. Thus, the separation of space into inner and outer regions naturally accommodates the possibility of an analytical or semianalytical description in the outer region. Correlation-induced coupling between different ionization and/or scattering channels in the outer region can also be included, for example, within first-order perturbation theory in correlations between the outgoing and core electrons. This is the subject of our companion paper [4], which looks at correlation-induced excitation of the ion during ionization [5,6].

In the context of using an analytical description for laser-driven dynamics in the outer region, we bring the reader's attention to the series of papers by A. Scrinzi and co-workers [7–10]. The numerical t-SURFF approach developed in these papers applies an *R*-matrix-type principle and uses Volkov states to propagate the continuum wave function in the outer region. Transfer onto the Volkov states is done at the boundary between inner and outer regions. Since Volkov states are exact solutions for the laser-driven continuum dynamics in the absence of interaction with the core, the boundary of the outer region has to be chosen beyond the range of the core potential. However, even for the long-range Coulomb potential, accurate results can be achieved with a very reasonable size of the inner region ($\sim$100 a.u.), turning off the interaction beyond the boundary. The major advantage of the method is that propagation in the outer region is fully analytic, making this approach computationally very efficient.

The introduction of inner and outer regions naturally leads to the idea of electron trajectories which enter and leave the inner region under the action of the strong laser field (see below). The wave function is naturally decomposed into a sum of components associated with a different number of returns into the inner region. From the perspective of the electron-ion recollision model in the strong laser field [11–13], the ARM formulation allows one to separate electron collisions with the parent ion into soft and hard. Soft collisions correspond to trajectories that stay outside the inner region; hard collisions correspond to those trajectories that cross into the inner region. With the dynamics built around semiclassical trajectories, hard collisions correspond to small impact parameters and lead to large-angle scattering. Following large-angle scattering, the scattered electron acquires high energy from the strong laser field and leaves the interaction region for good; a second hard collision is highly unlikely. Thus, the expansion of the wave function in the number of hard collisions should converge quickly.

The development of consistent approximations for the inner region must take into account the energy of the electron entering this region. During the ionization step, when the total electron energy is negative, the wave function in the inner region is dominated by the initial bound state, introducing a well-defined source term for the outer region. If the electron is driven back into the inner region by the laser field, one can rely on the fact that the electron spends only a short time in the inner region, and hence treat the effects of the laser field perturbatively during that time (see, e.g., [14]). To zeroth order, this treatment corresponds to the ansatz of so-called quantitative rescattering theory [15], which uses field-free scattering and/or recombination amplitudes and cross sections for describing the recollision step. Short scattering times justify this approach [14,16]. At the same time, such important effects in laser-driven recollision as Coulomb-laser coupling [17] and

laser-assisted Coulomb focusing [18] (which increase overall recollision cross sections by orders of magnitude [14]), absent in quantitative rescattering theory, can naturally be included as they are dominated by dynamics in the outer region. The ARM is also well suited for the description of strong-field driven time-resolved electron holography [19,21], which focuses on the interference of the strongly scattered object wave and the weakly scattered reference wave. The reference wave is the component of the wave function that stays in the outer region at all times. The object wave is the component of the wave function re-entering the inner region after ionization.

Finally, the emergence of electron trajectories originating from the inner region naturally suggests the application of semiclassical approaches in the spirit of techniques developed in [21–23]. In this context, one can use the analytical description of the wave packet created during the ionization step as the initial condition for trajectory-based techniques. The ionization step is challenging for trajectory-based methods as it often involves tunneling. The structure of the wave packet as it emerges from the classically forbidden region is analyzed in Sec. IV.

The paper is organized as follows: Section II outlines the main ideas and the basic formalism of the ARM. Section III applies this formalism to the canonical problem of strong field ionization from a Coulomb potential and compares results with the standard theory of Perelomov, Popov, and Terent'ev (PPT) [24]. Section IV analyzes the subcycle tunneling dynamics and shows how different momentum components of the tunneled wave packet are formed. Section V describes sublaser cycle effects associated with the long-range tail of the Coulomb potential, absent in standard PPT theory. Section VI concludes the paper.

II. BASIC FORMALISM AND APPROXIMATIONS

We partition the configuration space into an inner (1) and an outer region (2), separated along the boundary of a sphere with radius a [Fig. 1(a)]. Usually, dealing with laser-induced dynamics, one attempts to solve the initial value problem:

$$i\frac{\partial}{\partial t}\Psi(\mathbf{r},t) = \hat{H}\Psi(\mathbf{r},t), \tag{1}$$

$$\Psi(\mathbf{r},t=t_0) = \Psi_g(\mathbf{r}), \tag{2}$$

where $\hat{H}$ is the Hamiltonian of the system and Ψ_g is its ground state, where the system resides prior to the turning on of all laser pulses.

However, if we want to find a solution of Eq. (1) in the outer region (2), we have to take into account that, due to the presence of the boundary, the operator $\hat{H}$ is not Hermitian in both region (1) and region (2) separately [25] (see Appendix A; the culprit is the radial part $\hat{K}_r$ of the kinetic energy operator $\hat{K}$). Hermiticity is recovered if we compensate for the boundary terms which result from $\hat{K}_r$ acting in the half space. The compensation is achieved by adding the Bloch operator [1,25]

$$\widehat{L}^{\pm}(a) = \pm\delta(r-a)\hat{B}, \tag{3}$$

where the differential operator at the boundary in the r representation is

$$\hat{B} = \frac{d}{dr} + \frac{1-b}{r}. \tag{4}$$

Here, b is an arbitrary constant (which we later fix), and the δ function is defined such that

$$\int_a^\infty dr\,\delta(r-a) = \int_0^a dr\,\delta(r-a) = \frac{1}{2} \tag{5}$$

(see Appendix A for detailed discussion and derivation). The operator $\widehat{L}^{+}(a)$ makes the Hamiltonian Hermitian in the inner region, while $\widehat{L}^{-}(a) = -\widehat{L}^{+}(a)$ does the same for the outer region.

Thus, we rewrite the time-dependent Schrödinger equation (TDSE) as follows:

$$i\frac{\partial}{\partial t}\Psi(\mathbf{r},t) = [\hat{H} + \widehat{L}^{\pm}(a)]\Psi(\mathbf{r},t) - \widehat{L}^{\pm}(a)\Psi(\mathbf{r},t), \tag{6}$$

for the inner (+) and outer (−) region. We can now use the Bloch operator to reformulate Eq. (1) as a boundary problem [25]:

$$\begin{aligned} i\frac{\partial}{\partial t}\Psi(\mathbf{r},t) - \widehat{\mathcal{H}}^{(\pm)}\Psi(\mathbf{r},t) &= -\widehat{L}^{\pm}(a)\Psi(\mathbf{r},t) \\ &= \mp\delta(r-a)B(a,\theta,\phi,t), \\ B(a,\theta,\phi,t) &= \hat{B}\Psi(\mathbf{r},t)|_{r=a} \\ &= \left(\frac{d}{dr} + \frac{1-b}{r}\right)\Psi(\mathbf{r},t)|_{r=a}. \end{aligned} \tag{7}$$

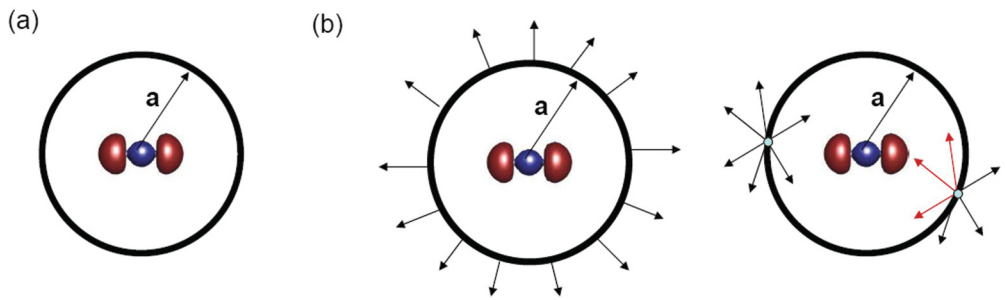

FIG. 1. (Color online) (a) Partitioning of the configuration space. (b) Schematic representation of the boundary condition for the exact Green's function (left) and the approximate eikonal-Volkov Green's function used in this paper (right). Note that the eikonal-Vokov approximation includes unwanted incoming solutions, indicated by the red arrows. However, in strong-field ionization problems, such pathways have to traverse the classically forbidden region to reach the origin. Therefore, they are strongly suppressed and introduce only exponentially small errors.

The Hermitian Hamiltonian $\widehat{\mathcal{H}}^{(+)} = \hat{H} + \widehat{L}^{+}(a)$ describes electron dynamics in the inner region, while in the outer region we have the Hermitian Hamiltonian $\widehat{\mathcal{H}}^{(-)} = \hat{H} + \widehat{L}^{-}(a) = \hat{H} - \widehat{L}^{+}(a)$. The solution of the inhomogeneous equation with the boundary condition Eqs. (7) can be written via the Green's function $\mathcal{G}^{a}(\mathbf{r},\mathbf{r}',t,t')$ of the corresponding homogenous equation. For the outer region we have

$$\Psi_{\rm out}(\mathbf{r},t) = -i\int d\mathbf{r}'\int_{-\infty}^{t} dt'\mathcal{G}^{a}_{\rm out}(\mathbf{r},t,\mathbf{r}',t') \times [-\widehat{L}^{-}(a)\Psi(\mathbf{r}',t')]_{r'=a}, \tag{8}$$

where the Green's function in the outer region,

$$\mathcal{G}^{a}_{\rm out}(\mathbf{r},t,\mathbf{r}',t') = \langle \mathbf{r}|e^{-i\int_{t'}^{t}\widehat{\mathcal{H}}^{(-)}d\tau}|\mathbf{r}'\rangle, \tag{9}$$

incorporates the boundary (note the Hamiltonian $\mathcal{H}^{(-)}$) and should describe waves outgoing from the boundary at t' [Fig. 1(b)]. Thanks to the localized action of the Bloch operator, the solution is obtained as long as we know the wave function $\Psi(\mathbf{r},t)_{r=a}$ and its derivative at any time t at the boundary $r = a$. Note that the required wave function at the boundary is exact and, formally, fully incorporates effects of the laser field. Equation (8) is complemented by the wave function in the inner region,

$$\Psi_{\rm in}(\mathbf{r},t) = -i\int d\mathbf{r}'\int_{-\infty}^{t} dt'\mathcal{G}^{a}_{\rm in}(\mathbf{r},t,\mathbf{r}',t') \times [-\widehat{L}^{+}(a)\Psi(\mathbf{r}',t')]_{r'=a} \tag{10}$$

with

$$\mathcal{G}^{a}_{\rm in}(\mathbf{r},t,\mathbf{r}',t') = \langle \mathbf{r}|e^{-i\int_{t'}^{t}\widehat{\mathcal{H}}^{(+)}d\tau}|\mathbf{r}'\rangle. \tag{11}$$

In the numerical implementation of the R-matrix approach, both time-independent [1] and the recently developed time-dependent method [26], the boundary of the sphere is taken rather far from the core. In our analytical work, however, we keep the boundary relatively close (the exact conditions will be defined later). We can then use Eqs. (8) and (10) to develop a series in the number of "crossings" of the boundary, leading to hard collisions.

First, the exact laser-dressed wave function at the boundary is approximated with its ground-state component, leading to the following solution in the outer region:

$$\Psi^{(1)}_{\rm out}(\mathbf{r},t) = i\int d\mathbf{r}'\int_{-\infty}^{t} dt'\mathcal{G}^{a}_{\rm out}(\mathbf{r},t,\mathbf{r}',t') \times [\widehat{L}^{-}(a)\psi_{g}(\mathbf{r}')]_{r'=a}a_{g}(t')e^{-iE_{g}t'}. \tag{12}$$

Here $a_g(t)$ includes the Stark shift of the field-free ground-state energy E_g and the decay of the norm of the ground-state component $\phi_g(\mathbf{r}')$ of the total wave function in the inner region. This approximation is reasonably far from saturation, when most of the wave function resides in the laser-polarized ground state. The expression is similar to the starting point of effective-range theory [27–29] for strong-field dynamics in short-range potentials, which are described by the effective boundary condition. The difference, however, is that here the wave function on the left-hand side of Eq. (12) is defined only outside the boundary.

In turn, $\Psi^{(1)}_{\rm out}(\mathbf{r},t)$ can be substituted into the equation for the inner region [Eq. (10)], describing the wave packet entering the inner region from the outside

$$\Psi^{(2)}_{\rm in}(\mathbf{r},t) = i\int d\mathbf{r}'\int_{-\infty}^{t} dt'\mathcal{G}^{a}_{\rm in}(\mathbf{r},t,\mathbf{r}',t')\big[\widehat{L}^{+}(a)\Psi^{(1)}_{\rm out}(\mathbf{r}',t')\big]_{r'=a}. \tag{13}$$

The next term in the series is $\Psi^{(3)}_{\rm out}(\mathbf{r},t)$, describing the wave packet that escapes into the outer region for the second time [$\Psi^{(1)}_{\rm out}(\mathbf{r},t)$ being the first]. Limiting the series to one "hard recollision" implies that it is terminated at $\Psi^{(2)}_{\rm in}(\mathbf{r},t)$ for the inner region and $\Psi^{(3)}_{\rm out}(\mathbf{r},t)$ for the outer region.

The utility of this series becomes clear when the semiclassical approximation is used for the propagators. Then tunneling is described by trajectories moving in complex time (see [24,30]). Once one is able to (i) introduce trajectories leaving the inner region for the first time in Eq. (12) and (ii) describe their motion through the classically forbidden region analytically, further evolution of these trajectories in real time can be described numerically without further partitioning the coordinate space into regions (1) and (2), incorporating the ionization step into the trajectory-based methods developed in [21,22].

Let us now replace $\mathcal{G}^{a}_{\rm out}$ in Eq. (8) by an approximate Green's function for the outer region. To this end, we use the eikonal-Volkov approximation (EVA) [2]. We have shown that the EVA propagator $\mathcal{U}^{\rm EVA}(t,T)$ is accurate for describing strong-field ionization for nonsingular core potentials $U(\mathbf{r})$ [3]. Thus, it is natural to apply it in the outer region. As Fig. 1(b) shows, unlike the true propagator, our approximation allows incoming as well as outgoing solutions at the boundary. However, in strong-field ionization such undesirable incoming pathways have to traverse an additional classically forbidden region. As a result, they decay exponentially and only introduce exponentially small errors in our calculations (see Appendix B).

The propagator $\mathcal{U}^{\rm EVA}(t,T)$ is constructed using the EVA to find eigenstates (quasienergy states) of the time-dependent Hamiltonian describing an arbitrary one-electron system bound by a potential $U(\mathbf{r})$ and interacting with a strong laser field $V_L(t) = \mathbf{r}\cdot\mathbf{F}(t)\cos(\omega t)$:

$$\hat{H} = \frac{\hat{\mathbf{p}}^2}{2} + U(\mathbf{r}) + \mathbf{r}\cdot\mathbf{F}(t)\cos(\omega t). \tag{14}$$

Here $\mathbf{F}(t) = \mathbf{F}f_L(t)$ includes the field envelope $f_L(t)$, $\mathbf{F}$ is the peak field strength, and ω is the laser field frequency. The EVA states $|\mathbf{p}^{\rm EVA}_T(t)\rangle$ are defined via backpropagation of field-free eikonal continuum states $|\mathbf{p}^{E}\rangle$ from time $t = T$ after the end of the laser pulse to time t, when the pulse is on:

$$\big|\mathbf{p}^{\rm EVA}_T(t)\big\rangle = \mathcal{U}^{\rm EVA}(t,T)|\mathbf{p}^{E}\rangle, \tag{15}$$

where $\mathcal{U}^{\rm EVA}(t,T)$ is the EVA propagator. The field-free states $|\mathbf{p}^{E}\rangle$ are characterized by their asymptotic momentum $\mathbf{p}$, and the superscript E in $|\mathbf{p}^{E}\rangle$ stands for "eikonal." In coordinate representation

$$\langle \mathbf{r}|\mathbf{p}^{E}\rangle = (2\pi)^{-3/2}e^{i\mathbf{p}\cdot\mathbf{r}}e^{iG_{0\mathbf{p}}(\mathbf{r})}, \tag{16}$$

where the $G_{0\mathbf{p}}(\mathbf{r})$ describes the distortion of the phase front, compared to the plane wave, at position $\mathbf{r}$. Equation (16) sets the initial condition for the propagation of EVA states at $t = T$.

The states are [2]

$$\langle \mathbf{r}|\mathbf{p}_T^{\mathrm{EVA}}(t)\rangle = \left[\frac{1}{(2\pi)^{3/2}} e^{\mathbf{i}(\mathbf{p}+\mathbf{A}(t))\cdot\mathbf{r} - \frac{\mathbf{i}}{2}\int_T^t d\tau[\mathbf{p}+\mathbf{A}(\tau)]^2}\right] \times e^{-i\int_T^t d\tau U(\mathbf{r}_L(\tau;\mathbf{r},\mathbf{p},t))} e^{\mathbf{i}G_{0\mathbf{p}}(\mathbf{r}_L(T;\mathbf{r},\mathbf{p},t))}. \quad (17)$$

The term in square brackets is the usual Volkov wave function, with the vector-potential $\mathbf{A}(t)$ defined as $\mathbf{F}(t) = -\frac{d}{dt}\mathbf{A}(t)$. In this paper we consider the laser field linearly polarized along the z axis. The next-to-last term in Eq. (17) represents the core potential-induced distortion of the phase front along electron trajectories in the laser field $\mathbf{r}_L$. The trajectory $\mathbf{r}_L(\tau) \equiv \mathbf{r}_L(\tau;\mathbf{r},\mathbf{p},t)$ starts at the point $\mathbf{r}$ at the moment t and is characterized by the asymptotic (canonical) momentum $\mathbf{p}$:

$$\mathbf{r}_L(\tau;\mathbf{r},\mathbf{p},t) = \mathbf{r} + \int_t^\tau dt''[\mathbf{p}+\mathbf{A}(t'')]. \quad (18)$$

The last term in Eq. (17) is associated with the phase distortion of the field-free states and ensures continuity of the solutions given by Eq. (17) at $t = T$. Improper choice of the initial condition would, in general, degrade the accuracy of the approximation [2]. However, if T is sufficiently large and the drift momentum of the electron is nonzero, $\mathbf{r}_L(T;a,\mathbf{p},t) \to \infty$ for $T \to \infty$ and $G_{0\mathbf{p}}(\mathbf{r}_L(T,\mathbf{r},\mathbf{p},t)) \to 1$, which is equivalent to substituting the eikonal initial condition by the plane wave at very large distances. The relevant distortion of the plane wave front is then accumulated under the combined action of both the core potential and the laser field, as the wave front is backpropagated towards the core.

Using the EVA states, we can write the following EVA Green's function:

$$G^{\mathrm{EVA}}(\mathbf{r},t,\mathbf{r}',t') = \langle \mathbf{r}|\mathcal{U}^{\mathrm{EVA}}(t,t')|\mathbf{r}'\rangle = \theta(t-t')\int d\mathbf{p}\langle \mathbf{r}|\mathbf{p}_T^{\mathrm{EVA}}(t)\rangle\langle \mathbf{p}_T^{\mathrm{EVA}}(t')|\mathbf{r}'\rangle. \quad (19)$$

This expression can then be substituted into Eq. (12) to calculate the wave function in the outer region. Thanks to the boundary nature of the Bloch operator, the trajectories $\mathbf{r}_L$ around which the EVA states and EVA propagator are built originate from the boundary. The approximation requires that they stay outside the inner region and hence describes only the so-called "direct" electrons, which do not experience hard recollisions with the core. The expression for $\Psi_{\mathrm{out}}^{(1)}(\mathbf{r},t)$ (12) using the EVA Green's function introduced above (19) can be effectively analyzed using the saddle-point method as we discuss below.

The ionization amplitude is obtained by projecting $\Psi_{\mathrm{out}}(\mathbf{r},t)$ on the field-free eikonal states $|\mathbf{p}^E\rangle$ in the same region:

$$a_{\mathbf{p}}(T) = \int_a d\mathbf{r}\langle \mathbf{p}^E|\mathbf{r}\rangle\Psi_{\mathrm{out}}(\mathbf{r},T), \quad (20)$$

where the $\int_a$ implies integration over the outer region only, which can be extended to all of space if the electron has left the inner region, for example, as $T \to \infty$. Since at $T \to \infty$ the electron wave packet is far from the core, projection onto the plane-wave continuum states is also adequate:

$$a_{\mathbf{p}}(T) = \int d\mathbf{r}\langle \mathbf{p}|\mathbf{r}\rangle\Psi_{\mathrm{out}}(\mathbf{r},T). \quad (21)$$

Substituting in G^{EVA} (19) in our expression for Ψ_{out} (8) and keeping in mind the orthogonality of the EVA states, the ionization amplitude becomes

$$a_{\mathbf{p}}(T) = -i\int^T dt' e^{-\frac{i}{2}\int_{t'}^T d\tau[\mathbf{p}+\mathbf{A}(\tau)]^2} \times \int \frac{d\mathbf{r}'}{(2\pi)^{3/2}} e^{-i\int_{t'}^T d\tau U[\mathbf{r}_L(\tau)]} e^{-i[\mathbf{p}+\mathbf{A}(t')]\cdot\mathbf{r}'} \times \delta(r'-a)\hat{B}\Psi_{\mathrm{in}}(\mathbf{r}',t'). \quad (22)$$

The expression for $a_{\mathbf{p}}(T)$ does not account for hard recollisions, but is well-suited for calculating the ionization yield, which is not affected by hard recollisions, and for the spectra of "direct" electrons.

III. STRONG FIELD IONIZATION: DERIVATION OF STANDARD RESULTS

The goal of this section is to both illustrate and test this approach. To this end, we derive ionization amplitudes in strong low-frequency fields. Our approach is most naturally used in the time domain. Thus, we shall look at the contribution to the ionization amplitude accumulated over a single half cycle of the laser pulse and then show how these results yield the standard results of PPT theory [24] developed for continuous laser radiation.

As mentioned before, we use the same approximation as [24] and replace the exact wave function at the boundary $\Psi(r'=a,t')$ with its ground-state component,

$$\Psi_{\mathrm{in}}(\mathbf{r}',t') \simeq e^{iI_p t'} a_g(t')\psi_g(\mathbf{r}'). \quad (23)$$

The Stark shift and depletion of the ground state should be incorporated into the amplitude $a_g(t)$, while $\psi_g(\mathbf{r})$ determines the spatial structure of the ground state [31]. To compare with standard PPT results for the Coulomb potential $U(r) = -Q/r$, we use the hydrogenic expression

$$\psi_g(\mathbf{r}) = \psi_{\kappa,l,m}(\mathbf{r}) = \varphi_{\kappa,l}(r)Y_{lm}(\theta,\phi) = \varphi_{\kappa,l}(r)N_{lm}P_l^m(\cos\theta)\frac{e^{im\phi}}{\sqrt{2\pi}}, \quad (24)$$

$$\varphi_{\kappa,l}(r) = C_{\kappa l}\kappa^{3/2}\frac{e^{-\kappa r}}{\kappa r}(\kappa r)^{Q/\kappa}, \quad (25)$$

$$N_{lm} = \sqrt{\frac{(2l+1)(l-m)!}{2(l+m)!}}. \quad (26)$$

Here $\kappa = \sqrt{2I_p}$ determines the size of the bound state $\sim 1/\kappa$, and $C_{\kappa l}$ is a constant.

Note that setting $b = Q/\kappa$ in Eq. (4) yields the simple result

$$\hat{B}\varphi_{\kappa,l}(r) = -\kappa\varphi_{\kappa,l}(r). \quad (27)$$

Before we commence our calculation of the ionization amplitude, let us first consider our choice of a, the radius of the sphere separating the inner and outer regions. At a, we would like to match a bound field-free solution in the inner region, with an outer solution that captures the laser field fully but treats the Coulomb interaction as a small correction. To do this successfully, a must lie inside the classically forbidden region, sufficiently far from both the entrance and the exit of the tunneling barrier. Specifically, to apply the eikonal

approximation, we must ensure that $a\kappa \gg 1$ or alternatively $|U(a)| \ll I_p$; that is, we are sufficiently far from the atom compared to the characteristic size of bound state and the Coulomb potential is no longer very important. On the other hand, the use of the field-free state in the inner region requires that $Fa \ll I_p$: The change in the electron energy due to the work of the electric field must be negligible compared to the energy of the bound state. Note that F/I_p roughly corresponds to the exit of the tunneling barrier (for sufficiently small values of the Keldysh parameter $\gamma = \omega\sqrt{2I_p}/F$). Putting this together, we require $1/\kappa \ll a \ll \kappa^2/2F$. Note that these conditions together impose an important restriction on the field strengths for which our analysis is justified, $F \ll \kappa^3$.

With approximation (23), the expression for the ionization amplitude Eq. (22) takes the form

$$a_{\mathbf{p}}(T) = \frac{i\kappa}{(2\pi)^{3/2}} \int^T dt' a_g(t') \int d\mathbf{r}' e^{-iS(T,t',\mathbf{r}',\mathbf{p})} \times \delta(r'-a)\varphi_{\kappa,l}(r')Y_{lm}(\theta,\phi), \tag{28}$$

where the phase of the integrand $S(T,t',\mathbf{r}',\mathbf{p})$ is determined by the action of a particle moving with canonical momentum $\mathbf{p}$ and having position $\mathbf{r}'$ at the moment t':

$$S(T,t',\mathbf{r}',\mathbf{p}) = \frac{1}{2}\int_{t'}^T d\tau[\mathbf{p}+\mathbf{A}(\tau)]^2 + \int_{t'}^T d\tau U[\mathbf{r}_L(\tau)] + [\mathbf{p}+\mathbf{A}(t')]\cdot\mathbf{r}' - I_p t'. \tag{29}$$

Energy is calculated relative to that of the ground state. We let the field $F\cos\omega t$ be linearly polarized along the z axis. The corresponding vector potential is

$$\mathbf{A}(t) = -\frac{F}{\omega}\sin\omega t\ \hat{\mathbf{e}}_{\mathbf{z}}. \tag{30}$$

A. Temporal integration

Using the δ function to evaluate the radial integral over r', we can rewrite the ionization amplitude as

$$a_{\mathbf{p}}(T) = \frac{i\kappa}{(2\pi)^{3/2}} a^2\varphi_{\kappa,l}(a)\, e^{-i\frac{p_\perp^2}{2}T} \times \int_0^\pi d\theta \int_0^{2\pi} d\phi\ \sin\theta\ Y_{lm}(\theta,\phi)\, e^{-iap_\perp\sin\theta\cos(\phi-\phi_p)} \times \int^T dt' a_g(t') e^{-iS_V(T,t',\mathbf{p})} e^{-i\sigma_U(t')} e^{-iv_z(t')a\cos\theta}, \tag{31}$$

where

$$S_V(T,t',\mathbf{p}) = \frac{1}{2}\int_{t'}^T d\tau\ v_z(\tau)^2 - I_{p,\mathrm{eff}}t', \tag{32}$$

$$I_{p,\mathrm{eff}} = I_p + \frac{p_\perp^2}{2}, \tag{33}$$

$$v_z(t') = p_\parallel + A(t'), \tag{34}$$

$$\sigma_U(t') = \int_{t'}^T d\tau U[\mathbf{r}_L(\tau;\theta,\mathbf{p},t')], \tag{35}$$

$p_\parallel = p_z$, $p_\perp^2 = p_x^2 + p_y^2$, and ϕ_p is the polar angle the momentum $p_\perp$ makes with the x axis. The contributions S_V and σ_U describe the Volkov part of the action and the correction from the core potential, respectively.

Fast oscillations of the phase in strong low-frequency fields allow one to use the saddle-point method to evaluate the integral over time. Such analysis can be done by treating the phase $\sigma_U(t')$ as a relatively slow function of t' and hence ignoring its contribution to the saddle points. This treatment is a natural first step within the eikonal approximation and proves accurate: The standard results of PPT theory are obtained using the saddle points found to zeroth order in $U(\mathbf{r}_L)$. Corrections to the saddle points can then be introduced perturbatively. Such an iterative treatment may further improve the original results of PPT theory, extending their applicability to the case of very large Keldysh parameter $\gamma = \omega\sqrt{2I_p}/F \gg 1$ as recently shown in [30].

We focus on the contribution from a half-cycle interval $-\pi/2 < \omega t < +\pi/2$, where $\cos\omega t' \geqslant 0$ and hence the electron should start moving in the negative-z direction.

Differentiating the phase with respect to t' and treating $\sigma_U(t')$ as slow compared to $S_V(t')$, we obtain the saddle-point equation, $\partial S/\partial t' = 0$:

$$\frac{1}{2}[p_\parallel + A(t')]^2 + \left[I_p + \frac{p_\perp^2}{2} + Fa\cos\theta\cos\omega t'\right] = 0. \tag{36}$$

Using this, we can approximate the solution as

$$a_{\mathbf{p}}(T) = \frac{i\kappa}{(2\pi)^{3/2}} a^2\varphi_{\kappa,l}(a) e^{-i\frac{p_\perp^2}{2}T} \times \int_0^\pi d\theta \int_0^{2\pi} d\phi\ \sin\theta\ Y_{lm}(\theta,\phi)\, e^{-iap_\perp\sin\theta\cos(\phi-\phi_p)} \times \frac{\sqrt{2\pi}\ a_g(t_a)}{\sqrt{|S_V''(t_a) + A''(t_a)a\cos\theta|}} \times e^{-iS_V(t_a)} e^{-i\sigma_U(t_a)} e^{-iv_z(t_a)a\cos\theta}, \tag{37}$$

where t_a solves Eq. (36).

There are a number of important observations. First, note that any deviation from the optimal tunneling direction $p_\perp = 0$ and $\cos\theta = -1$ leads to an increased effective I_p in Eq. (36) and therefore to an exponentially increased cost for tunneling. Consequently, tunneling will be dominated by small perpendicular momenta and angles $\theta \sim \pi$. We shall come back to this fact when we integrate over the surface of our sphere $r' = a$.

Second, recall that the use of the unperturbed ground state in the inner region requires that $Fa \ll I_p$. The final term in Eq. (36) should therefore represent only a small correction to I_p. From this, we can deduce that the solution t_a must lie near the saddle point $t_s = t_i + i\tau_T$ determined by the equation

$$[p_\parallel + A(t_i + i\tau_T)]^2 = -[2I_p + p_\perp^2] = -2I_{p,\mathrm{eff}}. \tag{38}$$

This can be rewritten as

$$v_z(t_s) = p_\parallel - \frac{F}{\omega}\sin(\omega t_i + i\omega\tau_T) = \pm i\sqrt{2I_{p,\mathrm{eff}}} = \pm i\kappa_{\mathrm{eff}}. \tag{39}$$

For $\cos\omega t_i > 0$, $v_z(t_s) = -i\kappa_{\mathrm{eff}}$ is the correct choice, ensuring that the landscape of the imaginary phase in the vicinity of $t_s = t_i + i\tau_T$ with positive imaginary part indeed corresponds to the saddle, and vice versa for $\cos\omega t_i < 0$. This choice, in turn, leads to an exponentially small ionization amplitude and exponential decay of the outgoing wave function for complex

times and $|r'| > a$. We can summarize this as

$$v_z(t_s) = i\alpha\kappa_{\rm eff}, \tag{40}$$

where $\alpha = -\text{sign}(\cos\omega t_i)$.

In general, the solution for t_s is

$$\begin{aligned}
\phi_i &\equiv \omega t_i = \beta \arcsin\left(\sqrt{\frac{P-D}{2}}\right) + (n-1)\pi,\\
\phi_\tau &\equiv \omega\tau_T = \text{arcosh}\left(\sqrt{\frac{P+D}{2}}\right),\\
P &= \overline{p}_\parallel^2 + \gamma_e^2 + 1, \quad D = \sqrt{P^2 - 4\overline{p}_\parallel^2},
\end{aligned} \tag{41}$$

where $\gamma_e = \sqrt{2I_{p,\rm eff}}\omega/F$ is the Keldysh parameter [32] for the effective ionization potential, $\overline{p}_\parallel = p_\parallel/p_0$ is the momentum measured in units of $p_0 = F/\omega$, and $\beta = \text{sgn}(\sin\phi_i)$. The solution is given not only for the specific half cycle we have been focusing on, but also for other half cycles.

With this in mind, let us expand t_a in powers of $(Fa/I_{p,\rm eff})$ and write $t_a = t_s + \Delta t_a$. We find that

$$\Delta t_a = -i\alpha\frac{a}{\kappa_{\rm eff}}\cos\theta \tag{42}$$

solves Eq. (36) to first order in $(Fa/I_{p,\rm eff})$. Note that $a/\kappa_{\rm eff} \ll \kappa/2F < \tau_T$, so Δt_a represents only a small correction to t_s.

Thanks to the stationarity of S_V at t_s, the shift Δt_a of the complex saddle point only contributes at second order to the phase $S_V + v_z a\cos\theta$. Thus, keeping only terms linear in $(Fa/I_{p,\rm eff})$ and focusing on the half cycle where $\cos\omega t' \geqslant 0$, we have

$$S_V(t_a) + v_z(t_a)a\cos\theta \approx S_V(t_s) - i\kappa_{\rm eff}a\cos\theta. \tag{43}$$

To lowest order in $(Fa/I_{p,\rm eff})$, we can also approximate $S_V''(t_a) + A''(t_a)a\cos\theta \approx S_V''(t_s)$ and $a_g(t_a) = a_g(t_s)$. Finally, taking into account that $p_\perp^2/\kappa^2 \ll 1$, we have $\kappa_{\rm eff} \approx \kappa$.

B. Spatial integration

Given the above approximations, we can now rewrite the ionization amplitude (37) as

$$\begin{aligned}
a_{\mathbf{p}}(T) &= \frac{i\kappa}{(2\pi)^{3/2}}a^2\,\varphi_{\kappa,l}(a)\,\frac{a_g(t_s)}{\sqrt{|S_V''(t_s)|}}\,e^{-iS_V(t_s)}\,e^{-i\frac{p_\perp^2}{2}T}e^{im\phi_p}N_{l,m}\\
&\times\int_0^\pi d\theta\,\sin\theta\,P_l^m(\cos\theta)\,e^{-\kappa a\cos\theta}e^{-i\sigma_U(t_a,\theta)}\\
&\times\int_0^{2\pi} d\phi'\,e^{im\phi'}e^{-iap_\perp\sin\theta\cos\phi'}.
\end{aligned} \tag{44}$$

The integral over ϕ yields the Bessel function:

$$\int_0^{2\pi} d\phi'\,e^{-iap_\perp\sin\theta\cos\phi'+im\phi'} = 2\pi(-i)^m J_m(p_\perp a\sin\theta). \tag{45}$$

Now, to evaluate the remaining integral over θ, notice that the integrand contains the term $\exp[-\kappa a\cos\theta]$. If we recall the condition $\kappa a \gg 1$, we see that this naturally confines the integral to the vicinity of $\theta = \pi$, where the exponent has a maximum. Let us therefore change the integration variable from θ to $\theta' = \pi - \theta \ll 1$ and take small-angle expansions.

First, consider the Coulomb term, $\exp[-i\sigma_U]$. Keeping only the lowest order term in θ' in the argument of $U(\mathbf{r}_L)$ and assuming that $p_\perp$ is small, we can approximate $\mathbf{r}_L(\tau)$ with the optimal tunneling trajectory $z_L(\tau)$ starting at $\mathbf{r}' = -a\hat{\mathbf{e}}_\mathbf{z}$ with $p_\perp = 0$,

$$\mathbf{r}_L(\tau;\theta,\mathbf{p},t_a) \simeq z_L(\tau;-a,p_\parallel,t_a) = -a + \int_{t_a}^{\tau} dt''(p_\parallel + A(t'')). \tag{46}$$

For the remaining θ-dependent terms, we can use the following small-angle expansions (see [33] for Legendre polynomials [34]),

$$\begin{aligned}
J_m(p_\perp a\sin(\pi-\theta')) &\simeq \frac{(p_\perp a\theta'/2)^m}{\Gamma(m+1)},\\
P_l^m(\cos(\pi-\theta')) &\simeq (-1)^l\left(\frac{(l+m)!}{2^m m!(l-m)!}\right)(\theta')^m,\\
e^{-a\kappa\cos\theta} &\simeq e^{\kappa a}e^{-\kappa a\frac{\theta'^2}{2}}, \quad \sin(\pi-\theta') = \theta'.
\end{aligned} \tag{47}$$

Note that the above approximation works very well for $l = m = 0$ even for modest κa but starts to increasingly overestimate the integral for larger l,m, unless κa is sufficiently large. As discussed before, the competing limit $aF/I_p \ll 1$ implies that F/κ^3 must, in turn, be suitably small for both conditions on a to be simultaneously satisfied.

Using the above, we are now able to evaluate the integral over θ. If we take into account that

$$\begin{aligned}
\int_0^\pi d\theta\,\theta\left[\frac{\theta^2}{2}\right]^m e^{-\kappa a\theta^2/2} &\simeq \left[\frac{1}{\kappa a}\right]^{m+1}\\
\int_0^\infty e^{-t}t^m dt &= \left[\frac{1}{\kappa a}\right]^{m+1}\Gamma(m+1),
\end{aligned} \tag{48}$$

we obtain

$$\begin{aligned}
a_{\mathbf{p}}(T) \simeq{}& \frac{(-1)^{l+m}i^{m+1}}{\sqrt{|S_V''(t_s)|}}C_{lm}e^{im\phi_p}e^{-i\frac{p_\perp^2}{2}T}\left[\frac{p_\perp}{\kappa}\right]^m\\
&\times e^{-i\frac{1}{2}\int_{t_s}^T d\tau[p_\parallel+A(\tau)]^2 + iI_{p,\rm eff}t_s}a_g(t_s)\\
&\times\left[\varphi_{\kappa,l}(a)ae^{\kappa a}e^{-i\int_{t_a}^T d\tau U(-a+\int_{t_a}^\tau[p_\parallel+A(t'')]dt'')}\right],
\end{aligned} \tag{49}$$

where

$$C_{lm} = \frac{1}{2^m m!}\sqrt{\frac{(2l+1)(l+m)!}{4\pi(l-m)!}}. \tag{50}$$

C. Independence of the boundary

Had we used the exact wave function at the boundary [35], the smooth continuation of the wave function from the inner to the outer region would have been naturally expected. Equally automatic would have been the independence of ionization amplitudes on the position of the boundary. However, we have used an unperturbed wave function in the inner region while taking full account of the laser field in the outer region. Thus, the independence of the results on the position of the boundary is neither ensured nor obvious.

The expression in square brackets in Eq. (49),

$$F_{\kappa,l} = \varphi_{\kappa,l}(a)ae^{\kappa a}e^{-i\int_{t_a}^T d\tau U[-a+\int_{t_a}^\tau[p_\parallel+A(t'')]dt'']}, \tag{51}$$

contains the terms which still depend on the position of the boundary. Recalling the expression for the bound wave function $\varphi_{\kappa,l}(a)$ (25), this simplifies to

$$F_{\kappa,l} = C_{\kappa l}\kappa^{1/2}(\kappa a)^{Q/\kappa} e^{-i\int_{t_a}^{T} d\tau U[-a+\int_{t_a}^{\tau}[p_\parallel + A(t'')]dt'']}. \quad (52)$$

Note that both the remaining a-dependent terms are associated with the Coulomb potential. We now show that their combination is (approximately) a independent. We do this in a general way, applicable for any potential U.

First, note that the trajectory in the argument of U can be rewritten via t_s:

$$e^{-i\int_{t_a}^{T} d\tau U[-a+\int_{t_a}^{\tau}[p_\parallel + A(t'')]dt'']} = e^{-i\int_{t_a}^{T} d\tau U[\int_{t_s}^{\tau}[p_\parallel + A(t'')]dt'']}. \quad (53)$$

Now let us look at the Coulomb term in the bound wave function, $(\kappa a)^{Q/\kappa}$. This can be rewritten as

$$(\kappa a)^{\frac{Q}{\kappa}} = e^{\frac{Q}{\kappa}\int_{1/\kappa}^{a}\frac{dz}{z}} = e^{-\frac{1}{\kappa}\int_{1/\kappa}^{a} U(z)dz}. \quad (54)$$

That is, the wave function contains the integral of the Coulomb potential between $z = 1/\kappa$ and the boundary. This asymptotic form is not special for the Coulomb potential, but is dictated by the general behavior of bound states in the classically forbidden region. The effective lower limit of the integral here is $z_\kappa = 1/\kappa$; for other potentials it could be different, but the general behavior is the same. For $z < 0$, relevant to our problem, the same applies:

$$(\kappa a)^{\frac{Q}{\kappa}} = e^{\frac{1}{\kappa}\int_{-1/\kappa}^{-a} U(z)dz}. \quad (55)$$

Keeping in mind that the electron velocity is $-i\kappa$, we can rewrite the spatial integral as an integral in the time domain,

$$(\kappa a)^{\frac{Q}{\kappa}} = e^{-i\int_{t_\kappa}^{t_a} d\tau U[\int_{t_s}^{\tau}(-i\kappa)dt'']}, \quad (56)$$

where the lower limit of the outer integral is $t_\kappa = t_s + \Delta t_\kappa$,

$$\Delta t_\kappa = \frac{-1/\kappa}{-i\kappa} = -i\frac{1}{\kappa^2}. \quad (57)$$

Now we see that the product of the two potential-dependent terms is a independent, and we have

$$F_{\kappa,l} = C_{\kappa,l}\kappa^{1/2} e^{-i\int_{t_\kappa}^{T} d\tau U[\int_{t_s}^{\tau}[p_\parallel + A(t'')]dt'']}. \quad (58)$$

As is clear from the derivation, this result is general. The bound wave function in the region beyond the size of the bound state can always be written via the spatial integral of the core potential in this region, starting from some initial point, for the Coulomb potential equal to $1/\kappa$. The spatial integral across the inner region, at the boundary $a \gg 1/\kappa$, can then be rewritten as a time integral, keeping in mind that the electron velocity is nearly constant. Matching this integral to the corresponding time integral in the outer region is natural. The caveat is in the fact that electron motion in the outer region includes the laser field, while in the inner region this field was ignored. Thus, one has to watch for artifacts introduced by ignoring the effect of the laser field in the inner region, as we have done here.

D. Comparison with PPT results

The ionization amplitude we have just derived, computed for a single half cycle of the laser field and hence for a single "'ionization burst," is

$$a_{\mathbf{p}}(T) \simeq a_g(t_s)\left(\frac{(-1)^{l+m} i^{m+1}}{\sqrt{|S_V''(T,t_s)|}} C_{lm} e^{im\phi_p} e^{-i\frac{p_\perp^2}{2}T}\left[\frac{p_\perp}{\kappa}\right]^m C_{\kappa l}\kappa^{1/2}\right) \times \left[e^{-i\int_{t_\kappa}^{T} d\tau U(\int_{t_s}^{\tau} dt''[p_\parallel + A(t'')])}\right] e^{-i\frac{1}{2}\int_{t_s}^{T} d\tau [p_\parallel + A(\tau)]^2 + i I_{p,\mathrm{eff}} t_s}. \quad (59)$$

The first from the right is the familiar Keldysh exponent $\exp[-iS_V(T,t_s,\mathbf{p})]$ calculated for the specific momentum $\mathbf{p}$, identical to that in the standard theory. Note that $t_s = t_s(\mathbf{p}) = t_i(\mathbf{p}) + i\tau_T(\mathbf{p})$ is determined by the equation

$$p_\parallel - \frac{F}{\omega}\sin(\omega t_i + i\omega\tau_T) = \alpha i\sqrt{2I_{p,\mathrm{eff}}} = \alpha i\kappa_{\mathrm{eff}}, \quad (60)$$

where $\alpha = -\mathrm{sgn}(\cos\omega t_i)$.

The second term, in square brackets, is the contribution of the Coulomb potential. For the maximum of the momentum distribution $p = 0$, which corresponds to ionization at the peak of the oscillating field, it is identical to the familiar Coulomb correction of PPT theory [36,37]. In our derivation, the Coulomb correction is $\mathbf{p}$ dependent. Since different final momenta $\mathbf{p}$ can be associated with different moments of ionization within the laser half cycle, we have access to the subcycle dependence of the Coulomb corrections.

Finally, the leftmost group of terms, also in brackets, is related to the angular structure of the wave function and is common for ionization from both long-range and short-range potentials. Comparing it with PPT theory, we should keep in mind that our calculations are done in the time domain, and that our expression gives the contribution to $a(\mathbf{p})$ from a single ionization burst during one half cycle of the laser field. The results of PPT theory [24] are, on the other hand, derived for an infinitely long pulse. They provide the ionization rate as a sum over all multiphoton channels:

$$\Gamma^{\mathrm{PPT}} = \sum_n \Gamma_n^{\mathrm{PPT}},$$
$$\Gamma_n^{\mathrm{PPT}} = 2\pi\int d\mathbf{p}|F_n(p)|^2\delta\left(\frac{p^2}{2} - (n-n_0)\omega\right) = 2\pi p_n\int d\Omega|F_n(p)|^2,$$
$$E_n = \frac{p_n^2}{2} = (n-n_0)\omega. \quad (61)$$

Here $n_0 = \frac{I_p + 2U_p}{\omega}$ is the minimum number of absorbed photons.

To compare the two results, we should calculate the contribution to the n-photon peak, sandwiched between the energies $E_n \pm \omega/2$, during one laser half cycle. In PPT theory, this contribution is

$$w_n = \frac{\pi}{\omega}\Gamma_n^{\mathrm{PPT}} = \frac{2\pi^2}{\omega} p_n\int d\Omega|F_n(p)|^2, \quad (62)$$

where $d\Omega$ implies integration over solid angle. In our approach, the same quantity is

$$w_n = \int_{E_n-\omega/2}^{E_n+\omega/2} d\mathbf{p}|a_{\mathbf{p}}(T)|^2 \simeq \omega p_n \int d\Omega |a_{\mathbf{p}}(T)|^2|_{p=p_n}. \quad (63)$$

Thus, the connection between the two results should be

$$|a_{\mathbf{p}}(T)|^2 = \frac{\omega^2}{2\pi^2}|F_n(\mathbf{p})|^2, \quad (64)$$

for $\mathbf{p}^2/2 = p_n^2/2$, where $|F_n(p)|^2$ is given by Eq. (53) of [24]. This is indeed the case, up to notation.

IV. SUBCYCLE IONIZATION DYNAMICS AND THE STRUCTURE OF THE TUNNELING WAVE PACKET

Our approach gives insight into the instantaneous ionization dynamics and the shape of the electronic wave packet as it tunnels. Let us analyze how the ionization amplitudes Eq. (59) are formed. First, we rewrite this result in a more compact form,

$$a_{\mathbf{p}}(T) = a_g(t_s)R_{\kappa lm}(\mathbf{p})e^{-i\int_{t_\kappa}^{T} d\tau U(\int_{t_s}^{\tau} dt''[\mathbf{p}+\mathbf{A}(t'')])} \times e^{-\frac{i}{2}\int_{t_s}^{T} d\tau[\mathbf{p}+\mathbf{A}(\tau)]^2 + iI_p t_s}, \quad (65)$$

where we have restored the full momentum dependence in the Coulomb term. The prefactor

$$R_{\kappa lm}(\mathbf{p}) = \frac{(-1)^{l+m} i^{m+1}}{\sqrt{|S_V''(T,t_s)|}} C_{lm} e^{im\phi_p} \left[\frac{p_\perp}{\kappa}\right]^m C_{\kappa l}\kappa^{1/2} \quad (66)$$

encodes the impact of angular structure of the ionizing state on ionization. The prefactor $R_{\kappa lm}(\mathbf{p})$ also appears in the analysis of Murray *et al.* for static fields [20]. This work shows how the static approach developed in [20] extends to oscillating fields.

The wave function at time T, determined by these amplitudes, represents the wave packet $|\Delta\Psi(T)\rangle$ associated with a single ionization burst around one of the instantaneous maxima of the oscillating laser field,

$$|\Delta\Psi(T)\rangle = \int d\mathbf{p}\, a_{\mathbf{p}}(T)\, |\mathbf{p}\rangle. \quad (67)$$

Since the EVA wave functions $|\mathbf{p}_T^{\mathrm{EVA}}(t)\rangle$ are approximate solutions of the TDSE in the outer region, we can use them to propagate the wave packet Eq. (67) backward in time until some moment t, yielding $|\Delta\Psi(t)\rangle$. This is, of course, only possible as long as the electron trajectories in the argument of $U(\cdots)$ stay outside the inner region. We can then project the result of this propagation on the plane wave basis $|\mathbf{p}+\mathbf{A}(t)\rangle$, gaining insight into the momentum composition of the wave packet after it emerges in the continuum.

This procedure yields the expression

$$a_{\mathbf{p}}(t) \equiv \langle \mathbf{p}+\mathbf{A}(t)|\Delta\Psi(t)\rangle = \langle \mathbf{p}+\mathbf{A}(t)| \int d\mathbf{k}\, a_{\mathbf{k}}(T)\left|\mathbf{k}_T^{\mathrm{EVA}}(t)\right\rangle$$
$$= \frac{1}{(2\pi)^3}\int d\mathbf{r}e^{-i\mathbf{p}\mathbf{r}}\int d\mathbf{k}e^{i\mathbf{k}\mathbf{r}}a_g(t_s)R_{klm}(\mathbf{k})e^{iI_p t_s} \times e^{-\frac{i}{2}\int_{t_s}^{t}[\mathbf{k}+\mathbf{A}(t'')]^2 dt''}e^{-iW_c(t,\mathbf{r},\mathbf{k},T)}, \quad (68)$$

where the term associated with the core potential is

$$W_c = \int_T^t U(\mathbf{r}_L(\tau;\mathbf{r},\mathbf{k},t))d\tau + \int_{t_\kappa}^{T} d\tau U\left(\int_{t_s}^{\tau} dt''[\mathbf{k}+\mathbf{A}(t'')]\right). \quad (69)$$

Notice that the two integrals in Eq. (68) are very nearly direct and inverse Fourier transforms. It is only the r dependence of W_c which prevents this from being the case.

In particular, the first term in Eq. (69) contains the trajectory $\mathbf{r}_L(\tau;\mathbf{r},\mathbf{k},t)$, which is characterized by canonical momentum $\mathbf{k}$ at infinity and coordinate $\mathbf{r}$ at the moment t. Integration over $\mathbf{r}$ means that all trajectories are sampled. In contrast, only a single trajectory $\mathbf{r}_L(\tau;0,\mathbf{k},t_s)$ appears in the argument of the second integral. This starts at t_s at the origin. As we will see, evaluating the integrals in Eq. (68) using the saddle-point (stationary phase) method will select precisely the trajectory that matches $\mathbf{r}_L(\tau;0,\mathbf{k},t_s)$ in the first term.

Let us now evaluate $a_{\mathbf{p}}(t)$ in the case $m=0$ by applying the saddle-point method to both $\mathbf{r}$ and $\mathbf{k}$ integrals simultaneously. The integrand contains $\exp[-i\Theta(\mathbf{r},\mathbf{k})]$, where

$$\Theta(\mathbf{r},\mathbf{k}) = \frac{1}{2}\int_{t_s}^{t}[\mathbf{k}+\mathbf{A}(t'')]^2 dt'' - \mathbf{k}\cdot\mathbf{r} + \mathbf{p}\cdot\mathbf{r} + W_c(t,\mathbf{r},\mathbf{k},T), \quad (70)$$

and to zeroth order with respect to W_c, we have the following saddle-point equations:

$$\frac{\partial}{\partial\mathbf{k}}\Theta(\mathbf{r},\mathbf{k})|_{\mathbf{r}_s,\mathbf{k}_s} = \int_{t_s}^{t}[\mathbf{k}_s+\mathbf{A}(t'')]dt'' - \mathbf{r}_s = 0,$$
$$\frac{\partial}{\partial\mathbf{r}}\Theta(\mathbf{r},\mathbf{k})|_{\mathbf{r}_s,\mathbf{k}_s} = \mathbf{p}-\mathbf{k}_s = 0. \quad (71)$$

Note that even though $t_s = t_s(\mathbf{k})$, the phase is stationary with respect to t_s and hence $\partial/\partial t_s$ does not contribute here. These equations select a unique trajectory in the final expression for $a_{\mathbf{p}}(t)$,

$$\mathbf{r}_s(\mathbf{p},t) = \mathbf{r}_L(t;0,\mathbf{p},t_s) = \int_{t_s}^{t}[\mathbf{p}+\mathbf{A}(t'')]dt'', \quad (72)$$

and lead to the following simple expression for the Coulomb term:

$$W_c(r_s(\mathbf{p},t)) = \int_{t_\kappa}^{t} d\tau U\left(\int_{t_s}^{\tau} dt''[\mathbf{p}+\mathbf{A}(t'')]\right). \quad (73)$$

Thus, within the saddle-point method, the amplitude can be approximated as

$$a_{\mathbf{p}}(t) \simeq a_g(t_s)e^{-iW_c(r_s(\mathbf{p},t))}e^{iI_p t_s} \times \frac{1}{(2\pi)^3}\int d\mathbf{r}e^{-i\mathbf{p}\cdot\mathbf{r}}\int d\mathbf{k}e^{i\mathbf{k}\cdot\mathbf{r}}R_{kl0}(\mathbf{k})e^{-\frac{i}{2}\int_{t_s}^{t}[\mathbf{k}+\mathbf{A}(t'')]^2 dt''}, \quad (74)$$

which leads to the final result

$$a_{\mathbf{p}}(t) \simeq a_g(t_s)e^{-iW_c(\mathbf{r}_s(\mathbf{p},t))}e^{iI_p t_s}R_{kl0}(\mathbf{p})e^{-\frac{i}{2}\int_{t_s}^{t}[\mathbf{p}+\mathbf{A}(t'')]^2 dt''}. \quad (75)$$

This expression is applicable for all times t as long as the saddle point $t_s = t_s(p)$ of the original time integral is fully passed. Note that for $t = T$, this expression is, in fact, identical to $a_{\mathbf{p}}(T)$, the ionization amplitude we derived for large T

[Eq. (65)]. It is also applicable along the contour connecting the complex saddle point $t_s = t_i + i\tau_T$ to the point t_i on the real time axis. Thus, it allows us to analyze how the amplitudes and the wave packet $\Delta\Psi$ are formed during tunneling.

For this purpose, it is useful to study the integrals in Eq. (68) in more detail. In particular, let us now evaluate $a_{\mathbf{p}}(t)$ by first integrating over $\mathbf{k}$ and then over $\mathbf{r}$. This analysis also illustrates a technical issue related to the applicability of the saddle-point (stationary phase) analysis to the double integral, given that the $\mathbf{r}$ integral on its own does not appear to contain fast-oscillating terms.

Again, we set the magnetic quantum number $m = 0$. Hence, $R_{\kappa,l,m}$ is independent of $k_\perp$. Applying the stationary phase method to the $\mathbf{k}$ integral in Eq. (68), we obtain the stationary phase equation

$$\int_{t_s}^{t} [\mathbf{k} + \mathbf{A}(t'')]dt'' - \mathbf{r} = 0, \tag{76}$$

which determines the stationary momentum $\mathbf{k}_s = \mathbf{k}_s(\mathbf{r})$,

$$\mathbf{k}_s = \frac{\mathbf{r} - \int_{t_s}^{t} \mathbf{A}(t'')dt''}{t - t_s}. \tag{77}$$

The result of $\mathbf{k}$ integration is

$$a_{\mathbf{p}}(t) \simeq \int d\mathbf{r} \left(a_g(t_s) \frac{R_{\kappa l 0} e^{-iW_c - i\pi/4 + iI_p t_s}}{[2\pi(t - t_s)]^{3/2}} \right) \times e^{-i\mathbf{p}\cdot\mathbf{r}} e^{i\mathbf{k}_s\cdot\mathbf{r}} e^{-\frac{i}{2}\int_{t_s}^{t} [\mathbf{k}_s + \mathbf{A}(t'')]^2 dt''}. \tag{78}$$

Using our expression for $\mathbf{k}_s$ and completing the square in the exponent, we can rewrite this as

$$a_{\mathbf{p}}(t) \simeq \int d\mathbf{r} \left(a_g(t_s) \frac{R_{\kappa l 0} e^{-iW_c - i\pi/4 + iI_p t_s}}{[2\pi(t - t_s)]^{3/2}} \right) \times e^{\frac{i}{2}\frac{(\mathbf{r} - \mathbf{r}_s(\mathbf{p},t))^2}{(t - t_s)}} e^{-\frac{i}{2}\int_{t_s}^{t} (\mathbf{p} + \mathbf{A}(t''))^2 dt''}, \tag{79}$$

where we have defined

$$\mathbf{r}_s(\mathbf{p},t) \equiv \int_{t_s}^{t} [\mathbf{p} + \mathbf{A}(t'')]dt''. \tag{80}$$

First, this expression clearly justifies the application of the saddle-point method for integration over $\mathbf{r}$. Second, it shows that during its motion in the classically forbidden region, when times are complex-valued, $t - t_s = -i\xi$, the wave packet is a Gaussian $\exp[-(\mathbf{r} - \mathbf{r}_s(\mathbf{p},t))^2/2\xi]$ that surrounds the trajectory $\mathbf{r}_s(\mathbf{p},t)$ and spreads as $(t - t_s)^{-3/2}$. This explains why a single trajectory can be used to evaluate the contribution of the core potential to the ionization amplitude as we discussed before. It also indicates how each momentum component $a_{\mathbf{p}}$ is formed. In particular, we see that each momentum component after tunneling can be associated with a Gaussian wave packet emerging from the classically forbidden region and then spreading. Note that we can now apply the stationary phase method to the integral over $\mathbf{r}$, reproducing the result (75) for $a_{\mathbf{p}}(t)$.

V. SUBCYCLE COULOMB EFFECTS

Trajectory-based techniques for strong-field ionization use quantum ionization amplitudes as input for ensembles of trajectories [21,22], which are then propagated classically. So far, the subcycle dynamics of the interaction between the departing electron and the core during tunneling has been ignored. The Coulomb effects in ionization are evaluated along a trajectory departing at the maximum of the oscillating laser field. This is an excellent approximation for the total ionization yield, even for large Keldysh parameter γ [30]. However, for problems such as high harmonic generation, where trajectories leaving the core after the instantaneous maximum of the oscillating field are very important, including those starting substantially past the maximum (short trajectories), such an approximation is not necessarily adequate. Our analysis allows us to evaluate the subcycle role of the Coulomb potential for instantaneous ionization amplitudes. We assume that $p_\perp = 0$.

The subcycle contribution from the Coulomb potential is given by $\exp[-iW_c]$, where

$$W_c(p) = \int_{t_\kappa}^{t} d\tau U \left(\int_{t_s}^{\tau} dt'' [p_\parallel + A(t'')] \right) \tag{81}$$

is evaluated along the complex-valued trajectory that starts at the origin at $t_s(p_\parallel) = t_i(p_\parallel) + i\tau_T(p_\parallel)$. Integration over τ is performed from t_κ until t. We choose our integration contour such that it has two sections. Its first leg starts at $t_\kappa = t_i + i\tau_T - i/\kappa^2$ and descends parallel to the imaginary time axis, until it hits t_i on the real time axis. The second leg continues along the real time axis from t_i to t (see Fig. 2).

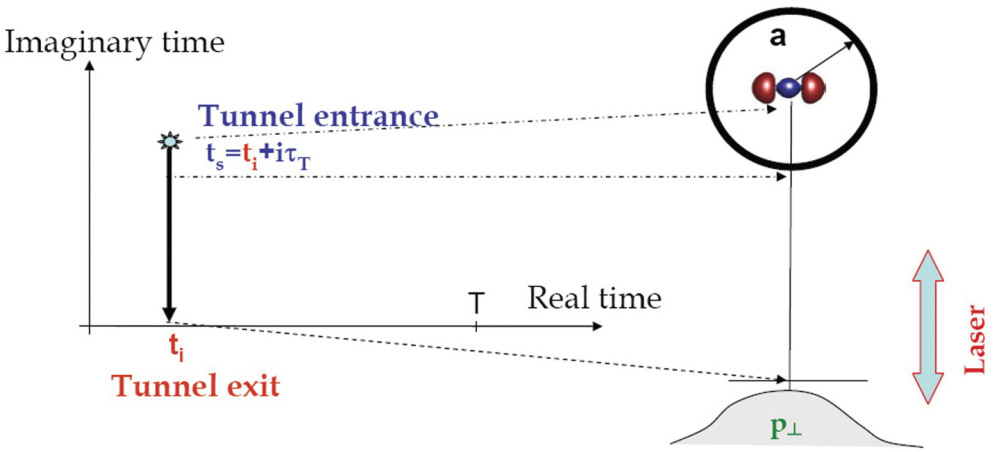

FIG. 2. (Color online) The integration contour for integral Eq. (81) and its relation to the boundary of the outer region.

While for the instantaneous maximum of the laser field $F\cos\omega t$ the trajectory is real-valued, in general it is complex. Therefore, the Coulomb potential should be analytically continued to the complex plane. In particular, $V_C(x) = -Q/|x|$ is continued as $V_C(x+iy) = -Q/\sqrt{(x+iy)^2} = -\mathrm{sgn}(x)Q/(x+iy)$.

We focus here on the imaginary part of the Coulomb phase which is responsible for the contribution to the ionization rate. For the maximum of the field, the imaginary part is accumulated only along the first section of the integration contour. In general, however, both sections contribute. In particular, the Coulomb correction to the ionization probability $|a_{\mathbf{p}}(t)|^2$ can be written as $e^{2W_{C1}+2W_{C2}}$, where

$$W_{C1} = \frac{Q}{\omega}\int_0^{\phi_\kappa} \frac{|r_1'|\,d\phi}{r_1'^2 + r_1''^2}, \tag{82}$$

$$W_{C2} = \frac{Q}{\omega}\int_{\phi_i}^{\omega t} \mathrm{sgn}(r_2')\,\frac{r_2''\,d\phi'}{r_2'^2 + r_2''^2}. \tag{83}$$

Here we have introduced dimensionless times $\phi_\kappa = \omega\tau_\kappa = \omega(\tau_T - 1/\kappa^2)$, $\phi_\tau = \omega\tau_T$, and $\phi_i = \omega t_i$ and the imaginary r'' and real r' parts of electron trajectories along the two sections of the integration contour:

$$r_1' = \alpha\frac{F}{\omega^2}|\cos\phi_i|\,(\cosh\phi_\tau - \cosh\phi)\,,$$

$$r_1'' = \beta\frac{F}{\omega^2}|\sin\phi_i|(\,\sinh\phi_\tau - \sinh\phi + \cosh\phi_\tau(\phi - \phi_\tau)),$$

$$r_2' = \frac{F}{\omega^2}\left[\cos\phi - \cos\phi_i\cosh\phi_\tau + \sin\phi_i\cosh\phi_\tau(\phi - \phi_i)\right],$$

$$r_2'' = \beta\frac{F}{\omega^2}|\sin\phi_i|\left[\sinh\phi_\tau - \phi_\tau\cosh\phi_\tau\right]. \tag{84}$$

Here, $\alpha = -\mathrm{sgn}(\cos\phi_i)$ and $\beta = \mathrm{sgn}(\sin\phi_i) = \mathrm{sgn}(p_{||})$. α is related to the sign of the electric field at the moment of ionization and gives the direction of electron escape. On the other hand, β encodes the sign of the electron's drift momentum.

Note that there are two possible scenarios here. If $\alpha = \beta$, the electron escapes in the negative (positive) z-direction with negative (positive) drift velocity and does not return to the core. This occurs for ionization times $\phi_i \in (-\pi/2,0),(\pi/2,\pi),\ldots$, that is, for ionization when the barrier is "opening". On the other hand, if $\alpha \neq \beta$ and the barrier is "closing", the electron emerges with a drift velocity back towards the ion. Such electrons will re-encounter the parent ion, and to treat this, we would need to account for recollisions. Here, we consider direct electrons only and hence restrict our attention to the first case. Note that in this instance $\mathrm{sgn}(r_2') = \alpha = \beta$.

Let us now consider the Coulomb correction terms, W_{C1} and W_{C2}, in more detail. The first correction [Eq. (82)] is always positive and therefore increases the ionization rate compared to the short-range potential. It is equal to:

$$W_{C1} = \int_0^{\phi_\kappa} d\phi \frac{(Q\omega/F)|\cos\phi_i|\,(\cosh\phi_\tau - \cosh\phi)}{\cos\phi_i{}^2\left[\cosh\phi_\tau - \cosh\phi\right]^2 + \sin\phi_i{}^2\left[\sinh\phi_\tau - \sinh\phi + \cosh\phi_\tau(\phi - \phi_\tau)\right]^2}. \tag{85}$$

This correction changes weakly within the cycle.

The subcycle dynamics of the second correction (accumulated along the real time axis) depend on whether the drift velocity is directed towards or away from the ion:

$$W_{C2} = \int_{\phi_i}^{\omega t} d\phi\ \mathrm{sgn}(r_2')\beta\,\frac{(Q\omega/F)|\sin\phi_i|[\sinh\phi_\tau - \phi_\tau\cosh\phi_\tau]}{[\cos\phi + \cosh\phi_\tau[(\phi - \phi_i)\sin\phi_i - \cos\phi_i]]^2 + \sin\phi_i{}^2\,(\sinh\phi_\tau - \phi_\tau\cosh\phi_\tau)^2}. \tag{86}$$

Note that, since $\phi_\tau \geqslant 0$, $(\sinh\phi_\tau - \phi_\tau\cosh\phi_\tau)$ is always negative. For direct ionization ($\alpha = \beta = \mathrm{sgn}(r_2')$), we therefore have $W_{C2} < 0$. That is, ionization is suppressed. This correction is intrinsically non-adiabatic. As the barrier is opening (becoming narrower), we can think of it as pulling the electrons back and causing additional trapping.

The nonadiabatic Coulomb correction $e^{2W_{C2}}$ does not affect electrons born around the maximum of the laser field (see Fig. 3). However, the probability of ionization for electrons born at the beginning of the ionization window is suppressed by about three times for typical experimental conditions.

VI. CONCLUSIONS

One of the key properties of our approach is its gauge invariance, as opposed to the standard methods based on the strong-field approximation (SFA). The difference between the results for ionization amplitudes calculated in the length and velocity gauges in the SFA originates from a combination of two factors. First, in the integral expressions for the ionization amplitude that serve as the starting point of the SFA theory, the initial bound state of the system is laser field free. That, in itself, is not an approximation as long as the final state is treated exactly. Second, the final continuum state is approximated by the Volkov state that ignores the effect of the core potential on the electron. This approximation brings the gauge noninvariance. The Volkov states are themselves gauge invariant in the sense that they yield gauge-independent answers for observables, as long as one is dealing with the free electron. However, they do contain the gauge-dependent factor in their spatial part: The spatial part is $\exp(i\mathbf{p}\cdot\mathbf{r})$ in the velocity gauge and $\exp\left(i(\mathbf{p} + \mathbf{A}(t))\cdot\mathbf{r}\right)$ in the length gauge. The factor $\exp\left(i\mathbf{A}(t)\cdot\mathbf{r}\right)$ disappears from all matrix elements where initial and final states are the Volkov states. However, in the SFA this difference cannot be compensated by the same gauge-dependent term in the initial state, since the latter is field free. In contrast, in our formulation the wave function in the inner region is exact, dressed by the laser field.

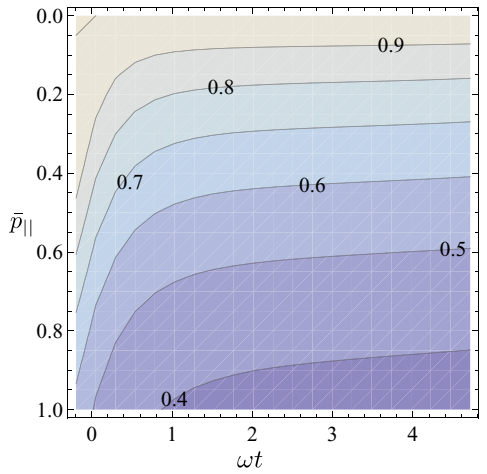

FIG. 3. (Color online) Nonadiabatic Coulomb correction $e^{2W_{C2}}$, plotted against time after ionization ωt, and scaled electron momentum, $\bar{p}_{||} = p_{||}/p_0$, $p_0 = F/\omega$. We consider only those electrons which leave in the negative z direction with negative momentum. This corresponds to ionization times $\phi_i \in (-\pi/2,0)$. Note that we must have $\omega t > \phi_i$. We assume an 800-nm laser field with intensity 1.3×10^{14} W/cm^2 and an ionization potential $I_p = 0.57$.

Therefore, transformation between length and velocity gauges will add the exact same gauge-related term to both bound and continuum states, compensating their contribution in the bound-free matrix element.

Our approach also demonstrates how the quasiclassical nature of tunneling in strong laser fields establishes a hierarchy of trajectories. Formally, the ionization amplitudes are determined by integrating over all $\mathbf{r}$ and hence over all trajectories. The interaction of the outgoing electron with the core incorporates all of them. However, the exponential cost of deviating from the optimal tunneling trajectory ensures that the tunneling wave packets associated with different ionization times have a Gaussian shape surrounding the optimal trajectory. Consequently, for each ionization time, the contributions from all possible trajectories to the interaction with the core are dominated by a single trajectory, which leaves the boundary between inner and outer regions along the direction of the field. The same conclusion will apply to effects associated with electron-electron correlation during ionization: the dynamic interaction of the outgoing electron with the electrons remaining in the core. These are the subject of the companion paper [4].

The formalism developed in this paper is naturally suited for multichannel ionization. Insight into the structure of the wave packet in complex time and the ability to evaluate the interaction of the core with the departing electron along characteristic tunneling trajectories are the key implications of our analysis. They show how the picture of non-interacting channels should be amended to include electron-electron correlation during tunneling.

ACKNOWLEDGMENTS

O.S. gratefully acknowledges DFG Grant No. Sm 292/2-1. L.T. acknowledges support from DiNL. O.S. and L.T. thank M. Ivanov for fruitful discussions.

APPENDIX A: DERIVATION OF THE BLOCH OPERATOR

To investigate the Hermiticity of the Hamiltonian H in the inner (outer) region we have to check that

$$C = \int d\mathbf{r}\Psi_1^*(\mathbf{r})(H\Psi_2(\mathbf{r})) - \int d\mathbf{r}(H\Psi_1(\mathbf{r}))^*\Psi_2(\mathbf{r}) = 0. \tag{A1}$$

Taking into account that the radial part of the Laplace operator has the form $\Delta = \frac{1}{r}\frac{d^2}{dr^2}r$, we obtain for the inner region

$$\begin{aligned} C &= \frac{1}{2}\int_0^a r^2 dr\Psi_1^*(\mathbf{r})\Delta\Psi_2(\mathbf{r}) - \frac{1}{2}\int_0^a r^2 dr\Delta\Psi_1^*(\mathbf{r})\Psi_2(\mathbf{r}) \\ &= \frac{1}{2}(r\Psi_1^*(\mathbf{r}))'\Psi_2(\mathbf{r})r|_0^a - \frac{1}{2}r\Psi_1^*(\mathbf{r})(\Psi_2(\mathbf{r})r)'|_0^a \\ &= \frac{1}{2}a^2(\Psi_1'^*(a)\Psi_2(a) - \Psi_1^*(a)\Psi'_2(a)) \neq 0. \end{aligned} \tag{A2}$$

Thus, to compensate the boundary terms we should add the Bloch operator to the Hamiltonian:

$$\widehat{L}^+(a) = \delta(r-a)\left(\frac{d}{dr} + \frac{1-b}{r}\right). \tag{A3}$$

Indeed,

$$\begin{aligned} &\int_0^a r^2 dr\Psi_1^*(\mathbf{r})L^+(a)\Psi_2(\mathbf{r}) \\ &\quad = \frac{1}{2}\Psi_1^*(a)\Psi'_2(a)a^2 + \frac{1-b}{2}\Psi_1^*(a)\Psi_2(a)a, \end{aligned} \tag{A4}$$

if we define our δ function such that $\int_0^a dr\delta(r-a) = \frac{1}{2}$. Note that the second term will always cancel with a corresponding term from the Hermitian conjugate, leaving us free to choose the constant b as we like.

To derive the Bloch operator for outer region we note that $\int_0^\infty dr = \int_0^a dr + \int_a^\infty dr$ and therefore for the outer region the Bloch operator differs only by sign:

$$\widehat{L}^-(a) = -\delta(r-a)\left(\frac{d}{dr} + \frac{1-b}{r}\right). \tag{A5}$$

It is possible to show that $\int_a^\infty dr\delta(r-a) = \frac{1}{2}$, and correspondingly $\int_0^a dr\delta(r-a) = \frac{1}{2}$, if $\delta(r-a) \equiv \frac{1}{2\pi}\int_{-\infty}^\infty dq e^{\mathbf{i}q(r-a)}$.

APPENDIX B: SOLUTION OF THE BOUNDARY PROBLEM FOR A TEST CASE

As an example, consider the simplest possible problem: that of a single state in a short-range potential. Our goal is to show that the approximation of using the full space Green's function, which does not incorporate the Bloch operator, to solve for the wavefunction in the outer region, leads to exponentially small errors.

Suppose we know the wave function of a particle at any moment of time at the boundary given by a sphere with radius $r = a$. In particular, consider $\Psi(a,t') = e^{iI_p(t'-t_0)}e^{-\kappa a}/a$, the solution for a short-range potential. We would now like to find the wave function of this particle outside the sphere for the Hamiltonian $H = \widehat{p}^2/2$ corresponding to free motion.

To this end, we would first have to find the outer region Green's function $\mathcal{G}^a(\mathbf{r},t,\mathbf{r}',t')$, which corresponds to

the Hamiltonian $H + \hat{L}^-(a)$ and satisfies the appropriate boundary conditions. However, instead, we shall simply use the Green's function $G(\mathbf{r},t,\mathbf{r}',t')$ for the Hamiltonian $H = \hat{p}^2/2$, given by:

$$G(\mathbf{r},t,\mathbf{r}',t') = \frac{1}{(2\pi)^3}\theta(t-t')e^{-\varepsilon(t-t')}\int d\mathbf{k}e^{i\mathbf{k}\cdot(\mathbf{r}-\mathbf{r}')}e^{-ik^2(t-t')/2}. \tag{B1}$$

where $\varepsilon \to 0$ and $\exp(-\varepsilon(t-t'))$ removes transient effects as $t - t' \to \infty$. This Green's function is defined on all of space, not just in the outer region. It propagates solutions outwards in all directions, and as a result, each point on the boundary effectively acts as a point source (see rightmost image in Fig. 1).

We shall now show that this approximation yields a solution with exponentially small errors if (i) the wave-function at the boundary corresponds to the bound state, (ii) the radius of the sphere is sufficiently large compared to the characteristic size of this bound state: $a\kappa \gg 1$, where $\kappa = \sqrt{2I_p}$ and $E = -I_p$ is the energy of this state.

To obtain an expression for $\Psi(\mathbf{r},t)$ using this Green's function, we have to insert a decomposition of unity over all of space, $\int d\mathbf{r}'|\mathbf{r}'\rangle\langle\mathbf{r}'|$,

$$\begin{aligned}\langle\mathbf{r}|\Psi(t)\rangle &= i\int_{-\infty}^{t} dt'\langle\mathbf{r}|e^{-i\hat{H}(t-t')}\hat{L}^-|\Psi_{\text{in}}(t')\rangle \\ &= i\int_{-\infty}^{t} dt'\int d\mathbf{r}'\langle\mathbf{r}|e^{-i\hat{H}(t-t')}|\mathbf{r}'\rangle\langle\mathbf{r}'|\hat{L}^-|\Psi_{\text{in}}(t')\rangle \\ &= i\int_{-\infty}^{t} dt'\int d\mathbf{r}' G(\mathbf{r},\mathbf{r}',t,t')\delta(r'-a)e^{iI_pt'}\kappa\frac{e^{-\kappa a}}{a},\end{aligned} \tag{B2}$$

where in the last line we have used the fact that $\langle\mathbf{r}'|\hat{L}^-|\Psi_{\text{in}}\rangle = \delta(r'-a)\kappa\Psi(a,t')$ if we choose b appropriately in our definition of $\hat{L}^-$.

Evaluating the integral over time t' first, we get

$$\Psi(\mathbf{r},t) = \frac{\kappa e^{iI_pt-\kappa a}}{a(2\pi)^3}\int d\mathbf{r}'\int d\mathbf{k}e^{i\mathbf{k}\cdot(\mathbf{r}-\mathbf{r}')}\frac{2}{\mathbf{k}^2+\kappa^2}. \tag{B3}$$

Now we integrate over $\mathbf{k}$. First, integrate over angular coordinates θ and ϕ between the vectors $\mathbf{r}-\mathbf{r}'$ and $\mathbf{k}$:

$$\begin{aligned}\int d\mathbf{k}\frac{1}{(2\pi)^3}\frac{2e^{i\mathbf{k}\cdot(\mathbf{r}-\mathbf{r}')}}{\kappa^2+k^2} &= \frac{-i}{4\pi^2|\mathbf{r}-\mathbf{r}'|}\int_0^\infty dk\frac{2k}{\kappa^2+k^2} \\ &\quad\times[e^{ik|\mathbf{r}-\mathbf{r}'|}-e^{-ik|\mathbf{r}-\mathbf{r}'|}].\end{aligned} \tag{B4}$$

Next, observe that the integrand is an even function of k and extend the limits of integration to $\pm\infty$,

$$\int_0^\infty dk\frac{k}{\kappa^2+k^2}[e^{ik|\mathbf{r}-\mathbf{r}'|}-e^{-ik|\mathbf{r}-\mathbf{r}'|}] = \int_{-\infty}^\infty dk\frac{k}{\kappa^2+k^2}e^{ik|\mathbf{r}-\mathbf{r}'|}. \tag{B5}$$

Now we can use the residue theorem and take the outgoing solution corresponding to the pole $k = i\kappa$, completing the integration contour in the upper half plane:

$$\int_{-\infty}^\infty dk\frac{2k}{\kappa^2+k^2}e^{ik|\mathbf{r}-\mathbf{r}'|} = \frac{2\pi i}{\kappa}e^{-\kappa|\mathbf{r}-\mathbf{r}'|}. \tag{B6}$$

Substituting these results into Eq. (B3) and performing spatial integration, we get

$$\Psi(\mathbf{r},t) = e^{iI_pt}\frac{e^{-\kappa r}}{r}(1-e^{-2\kappa a}). \tag{B7}$$

Thus, assuming $a\kappa \gg 1$, deviation from the exact result $\Psi(\mathbf{r},t) = e^{iI_pt}\frac{e^{-\kappa r}}{r}$ is exponentially small. The error term represents the contribution of the undesirable inwards moving solutions discussed above [the red arrows in Fig. 1(b)].

[1] P. G. Burke and J. Tennyson, Mol. Phys. **103**, 2537 (2005).
[2] O. Smirnova, M. Spanner, and M. Ivanov, Phys. Rev. A **77**, 033407 (2008).
[3] O. Smirnova, M. Spanner, and M. Ivanov, J. Phys. B **39**, S307 (2006).
[4] L. Torlina, M. Ivanov, Z. Walters, and O. Smirnova, following paper, Phys. Rev. A **86**, 043409 (2012).
[5] Z. Walters and O. Smirnova, J. Phys. B **43**, 161002 (2010).
[6] J. Eberly (private communication).
[7] A. Scrinzi (private communication).
[8] L. Tao and A. Scrinzi, New J. Phys. **14**, 013021 (2012).
[9] A. Scrinzi, Phys. Rev. A **81**, 053845 (2010).
[10] J. Caillat, J. Zanghellini, M. Kitzler, O. Koch, W. Kreuzer, and A. Scrinzi, Phys. Rev. A **71**, 012712 (2005).
[11] M. Yu. Kuchiev, Sov. Phys. JETP Lett. **45**, 404 (1987).
[12] P. B. Corkum, Phys. Rev. Lett. **71**, 1994 (1993).
[13] K. Kulander, in *Super-Intense Laser-Atom Physics Proceedings of a NATO ARW held in Han-sur-Lesse, Belgium, January 8–14, 1993*, edited by A. L'Huillier, Bernard Piraux, and Kazimierz Rzazewski, NATO Science Series B: Physics Vol. 316 (Kluwer, Dordrecht, 1993).
[14] G. L. Yudin and M. Yu. Ivanov, Phys. Rev. A **63**, 033404 (2001).
[15] A. T. Le, R. R. Lucchese, S. Tonzani, T. Morishita, and C. D. Lin, Phys. Rev. A **80**, 013401 (2009).
[16] M. V. Frolov, N. L. Manakov, T. S. Sarantseva, M. Y. Emelin, M. Y. Ryabikin, and A. F. Starace, Phys. Rev. Lett. **102**, 243901 (2009).
[17] O. Smirnova, A. S. Mouritzen, S. Patchkovskii, and M. Ivanov, J. Phys. B **40**, F197 (2007).
[18] T. Brabec, M. Y. Ivanov, and P. B. Corkum, Phys. Rev. A **54**, R2551 (1996).
[19] M. Spanner, O. Smirnova, P. B. Corkum, and M. Yu. Ivanov, J. Phys. B **37**, L243 (2004).
[20] R. Murray, M. Spanner, S. Patchkovskii, and M. Yu. Ivanov, Phys. Rev. Lett. **106**, 173001 (2011).
[21] Y. Huismans *et al.*, Science **331**, 61 (2011).
[22] S. V. Popruzhenko and D. Bauer, J. Mod. Opt. **55**, 2573 (2008).
[23] A. Kirrander and D. V. Shalashilin, Phys. Rev. A **84**, 033406 (2011).
[24] A. M. Perelomov, V. S. Popov, and M. V. Terent'ev, Sov. Phys. JETP **23**, 924 (1966).

[25] C. Bloch, Nucl. Phys. **4**, 503 (1957).
[26] L. R. Moore, M. A. Lysaght, J. S. Parker, H. W. van der Hart, and K. T. Taylor, Phys. Rev. A **84**, 061404 (2011).
[27] N. L. Manakov and L. P. Rapoport, Sov. Phys. JETP **42**, 430 (1975).
[28] M. V. Frolov, N. L. Manakov, E. A. Pronin, and A. F. Starace, Phys. Rev. Lett. **91**, 053003 (2003).
[29] M. V. Frolov, N. L. Manakov, E. A. Pronin, and A. F. Starace, J. Phys. B **36**, L419 (2003).
[30] S. V. Popruzhenko, V. D. Mur, V. S. Popov, and D. Bauer, Phys. Rev. Lett. **101**, 193003 (2008).
[31] In PPT theory $a_g(t)$ is omitted. It can be incorporated as shown in [3].
[32] L V Keldysh, Sov. Phys. JETP **20**, 1307 (1965).
[33] Alan Jeffrey and Daniel Zwillinger (eds.), *Gradshteyn and Ryzhik's Table of Integrals, Series, and Products*, 6th ed. (Academic Press, San Diego, 2000).
[34] The factor $(-1)^l$ accounts for the negative sign of the lobe of the electron wave function for $\theta = \pi$.
[35] The use of an approximate Green's function should introduce only an exponentially small error (see Appendix B).
[36] V. S. Popov, Phys. Usp. **42**, 733 (1999).
[37] A. Becker and F. Faisal, J. Phys. B **38**, R1 (2005).